Mitigating System's Voltage Instability Through Wide-Area Early Warning Signals and Real-Time HVDC Control

Kim Weyrich, Rujiroj Leelaruji, *Student Member, IEEE*,
Walter Kuehn, *Member, IEEE*, and Luigi Vanfretti, *Member, IEEE*

***Abstract*—Two sequential approaches to prevent voltage instability are proposed in this article. The first approach utilizes synchrophasors in order to establish when the system is leading to a voltage instability and also to trigger the operation of HVDCs to relieve the system's stress. The second approach is used to ensure that HVDCs will operate securely when their transfer is pushed towards the maximum transferable power level.**

***Index Terms*—Wide-Area Voltage Instability Detection, Classic HVDC, VDCOL, Automatic Voltage Stabilizer, Automatic Power Order Reduction**

I. Introduction

This article addresses the challenge of mitigation of voltage instability through two sequential approaches. First, voltage sensitivities computed from synchrophasor data can be used for system's voltage stability monitoring and exploited for delivering wide-area early action signals that can be used for prompting controllable devices such as HVDCs. In order to provide reliable information, synchrophasor data must be pre-processed to extract only the useful information, i.e. generation of warning signals. This warning signal can be used to trigger the operation of HVDCs before they reach stringent operating conditions.

The second approach considers cases when the operation boundaries need to be pushed to their limits. In this case, Classical HVDC systems are prone to voltage instability when operating on weak AC grids and to electromechanical transients when dealing with AC networks with multiple areas. In this article, a newly developed Automatic Voltage Stabilizer (AVS) and Automatic Power Order Reduction (APOR) controls are implemented in the CIGRÉ Benchmark Model for HVDC Controls to cope with these conditions in a real-time platform.

II. Wide-Area Voltage Stability Monitoring

An overall situational awareness can be achieved through the exploitation of synchrophasor measurements and other data [1], allowing to compute stress indices [2] and to determine the inception of instabilities [3]. For voltage stability monitoring, [3] proposes to track the sensitivities of a Jacobian matrix. In this article a similar approach is adopted, however a different Jacobian matrix from that of the standard power flow problem is utilized. The elements in this modified Jacobian matrix (2) are derived from the power flow in each transmission line. This means that the effects of shunt capacitances of the transmission line (in the case of medium and short lines) of the nominal π-model are also included.

The transmitted power on the line can be expressed as follows:

$$\begin{aligned} \overline{S}_{ik} &= V_i e^{j\delta_i}\{I_{ik}e^{j\delta_{ik}}\}^* \\ P_{ik} &= Re(\overline{S}_{ik}), \quad Q_{ik} = Im(\overline{S}_{ik}) \end{aligned} \tag{1}$$

where
V_i = voltage magnitude at Bus i.
I_{ik} = current magnitude from from Bus i to Bus k.
δ_i = voltage angle at Bus i.
$\delta_{ik} = \delta_i - \delta_k$.

$\overline{S}_{ik}$ = complex power transmitted from Bus i to Bus k.
P_{ik} = transmitted real power from Bus i to Bus k.
Q_{ik} = transmitted reactive power from Bus i to Bus k.

From (1) it follows that the real and reactive power flows through the transmission lines can be calculated directly from the measured voltage and current phasors regardless the system's parameters.

The modified Jacobian matrix can be constructed as follows:

$$J(\delta, V) = \begin{bmatrix} P_{ik_\delta}(t) & P_{ik_V}(t) \\ Q_{ik_\delta}(t) & Q_{ik_V}(t) \end{bmatrix} \tag{2}$$

where
$P_{ik_\delta}(t) = P_{ik}(t) - P_{ik}(t-1)/\delta_i(t) - \delta_i(t-1) = dP_{ik}/d\delta_i$
$P_{ik_V}(t) = P_{ik}(t) - P_{ik}(t-1)/V_i(t) - V_i(t-1) = dP_{ik}/dV_i$
Similar expressions can also be derived for Q_δ and Q_V.
The values of these sensitivities can aid in assessing voltage instability with the considerations below.

1) The sensitivities are consistently at a low-positive value (or negative depending the current measurement direction) with the assumption of steady-state operation. This indicates operation away from a voltage instability condition.
2) The value of the sensitivities will increase positively (or negatively) when a system is stressed. This denotes a system is moving towards a "weak" operating condition, this is a trend in the development of the voltage instability.
3) The value increases abruptly to very high positive (or negative) and switches sign in the case of a lack of reactive power support for dV_i/dQ_{ik} or when the maximum power transfer is reached for dV_i/dP_{ik}. This depicts an unstable condition which consequently leads to voltage collapse.

However, before computing sensitivities, the original voltages and current phasors must be filtered to remove fast dynamics and large outliers. Meanwhile, the start-up and ending transients can be eliminated by buffering data into a predefined finite-size window. The filtering process is applied

Invited Paper for the Panel Session: "RT and HIL Simulation for Approaching Complexity in Future Power & Energy Systems", 2012 IEEE Workshop on Complexity in Engineering, June 11-13, 2012. Aachen, Germany.

K. Weyrich and W. Kuehn are with the Department of EE & IT at FH Frankfurt University of Applied Sciences. E-mail: kim.weyrich@gmx.de, walter.kuehn@ieee.org

R. Leelaruji and L. Vanfretti are with the Electric Power Systems Division, School of Electrical Engineering, KTH Royal Institute of Technology, Teknikringen 33, SE-100 44, Stockholm, Sweden. E-mail: rujiroj@kth.se, luigiv@kth.se

to each window data, which is updated with each new sample. Finally, the ending transient of the filter is eliminated by using the last measured samples in a data buffer to maintain the window size. An additional step is to apply a moving average (MA) filter by computing the mean and standard deviation of the filtered signal. The size of the MA window is designed to cover the data which deviates from the mean value of the filtered signal, which originally has the same size as the predefined finite-size window as mentioned earlier. The MA aids to increase the robustness of the computed sensitivities. However, these filtering methods (either with or without moving average window) introduce a small delay to the calculation of sensitivities ($\approx$ 5 sec for this simulation).

To illustrate, a voltage instability scenario is conducted by gradually increasing constant active and reactive load models at Bus 5 of the test system shown in Fig. 1. Bus 3-to-Bus 5 transfers are considered here when the Bus 3 HVDC terminal is a rectifier. Figure 2 shows PV-curve of the system resulting from the load increase, and Fig 3 depicts the corresponding sensitivities (dV_5/dP_{53} and dV_5/dQ_{53}) calculated from unfiltered, filtered, filtered with MA.

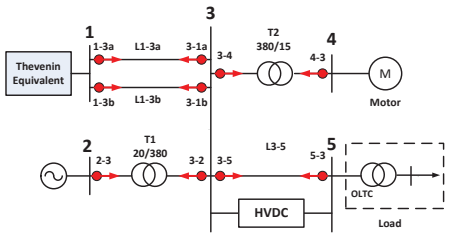

Fig. 1. Test system used for generating voltage instability scenarios

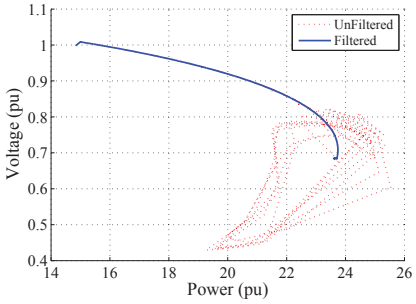

Fig. 2. Filtered and Unfiltered PV-curves computed at Bus 5 with the HVDC in operation (constant P_{dc} and Q_{dc} injection).

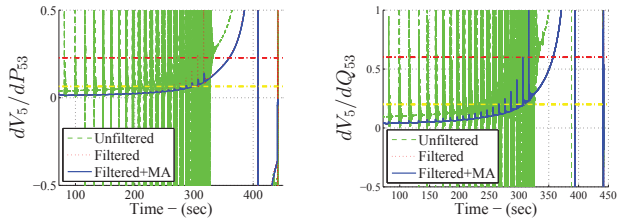

(a) dV_5/dP_{53} (b) dV_5/dQ_{53}

Fig. 3. Plot of calculated dV_5/dP_{53} and dV_5/dQ_{53} sensitivities calculated from filtered and unfiltered signals.

As seen from Fig. 2 and 3, proper filtering plays a vital role. A lack of and/or incorrect data processing can yield in incorrect information, which can result in an improper control action that could lead to a collapse. The spikes shown in the green in Fig. 3 correspond to OLTC tap position changes. It can also be noted that the sensitivity calculated from the unfiltered data (green dashed line) are vulnerable to OLTC tap switching and vary abruptly compared with those computed using data which has been filtered, or filtered with MA.

In addition, the sensitivities can be used to generate an early warning alarm when its value changes from positive to negative. This early warning alarm can be generated by setting a threshold value (which is pre-set through stability studies), hence allowing detection before the sensitivities change abruptly to a large positive value. Horizontal yellow and red dash-dot lines in Fig. 3 refer to an insecure and an emergency state, that have been pre-set, respectively. For instance, two thresholds for alarms are set for an early warning signal (yellow dash-dot line), and for a final alarm (red dash-dot line). The warning signal can be adopted to adjust the AC power transfer though HVDC power control before reaching dangerous conditions.

For reasons of simplicity and to keep the eye on fundamentals the HVDC model in Fig. 1 holds for VSC-HVDC, whereby the internal voltage of the inverter is synchronized with the AC system voltage via a PLL with low gain to implement virtual inertia. The HVDC model permits to control continuously active and reactive power injection through HVDC and to apply active power steps for determining transient effects at different operating points on the PV-curve. The closer the operating point to the stability boundary the higher the swings expressed through the size of the spiral trajectories Fig. 4. The reason for less damping when being closer to the stability boundary is that the synchronizing power goes down with decreasing stability margin. At the nose of the PV-curve this synchronizing power becomes zero, and it becomes negative when the nose of the PV-curve is surpassed. This happens simultaneously with the crossing of the maximum stable transmission angle. Then with negative damping the system becomes electromechanically unstable [4].

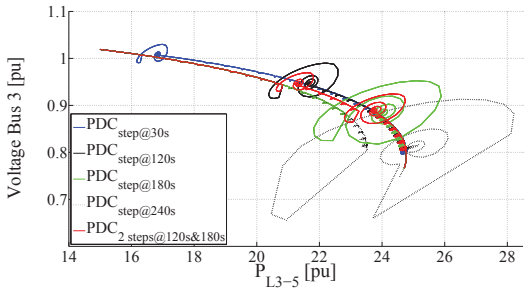

Fig. 4. Electromechanical swings in PV-curves due to DC power steps

Moreover, the requirement of DC power step change which was mentioned earlier can occur when a specific load demand changes due to an hourly-block in the electricity market, regardless of the system's operating point at that moment. This power step could be applied without severe consequences if and only if the HVDC is VSC-type and a parallel AC line in Fig. 1 is a short line and of about the same length as the HVDC. It is also important to note that the control mode of this VSC-HVDC is $P-Q$ control mode (i.e. the voltage control

mode is not adopted) due to a specific active and reactive load demand whereas the use of voltage control mode (with a proper design) can be used to avoid voltage stability problem but not necessarily transmission angle instability [5] .

In contrast, if the HVDC used in Fig. 1 is the Classical-type and is used to connect two grids which are, e.g., 1000 km apart, an increase of the DC active power will also increase the reactive power consumption of the converter. The effect of decreasing synchronizing power occurs definitely in more abrupt way when real converter controls for Classical HVDC are included. In this case voltage decline will mean: *a)* less reactive power generation through filter circuits and capacitors and *b)* longer commutation time due to lower commutation voltage and higher DC current increasing the reactive power consumption of the converter. It is obvious that for AC and Classical HVDC transmission systems operating in parallel high complexity governs the steady state and transient characteristics and performance of such systems [6]. The described relationships hold for both rectifier and inverter operation but the voltage decreasing relationships are particularly delicate for inverter operation. Commutation failures are likely to occur on the descending part of the HVDC PV-curve, i.e. when the extinction angle of the inverter reaches its minimum value. Commutation failures will occur before the PV-curve reaches the steady state stability boundary of a normal AC grid for which Fig. 4 holds. Hence, it is significantly important to know the power order to avoid this unstable process. A proper HVDC model and method to calculate the stability margin are required, this is reserved for later publication. Here a stabilizing method for Classical HVDC to prevent these undesired conditions is proposed in Section III where it is tested with different situations explained in Section IV. The method holds also for VSC-HVDC where transmission angle stability has to be ensured with either $P-Q$ or $P-V$ control regime [7].

III. The Proposed Classical HVDC Stabilizing Methods

As mentioned earlier, voltage supporting reactive power and synchronizing power keeping a two-area system synchronized diminish dramatically when at least one of the AC grids that HVDC is connected becomes weak (in other words, low Short-Circuit-Ratio (SCR)) due to switching off AC lines or reactive power supply limitations. In order to avoid voltage instability and power loss, certain operational measures are currently taken. Two important ones are event triggered power order reduction and voltage dependent current order limitation (VDCOL).

The first measure works reliably if the trigger signal is available for all probable events. This can only be ensured in a radial system while a meshed grid will be too complex to incorporate all forthcoming grid changes. With regards to the second measure which reduces the DC current order in response to decreasing AC or DC voltage (at the rectifier side), the problem lies in the difficulty to choose a suitable characteristic to reduce the DC current at a varying SCR. An AC grid with a normally high ratio requires a different characteristic when the ratio goes down. However, there is no automatic adaptation, voltage instabilities caused from HVDC itself may occur. These challenges can be solved by applying the Automatic Voltage Stabilizer (AVS) [7]. The AVS is based on an on-line steady state stability analysis using a dynamic stability limit detection method [5]. The PV-characteristic in Fig. 5 provides information about a generic AC transmission system with regards to voltage instability.

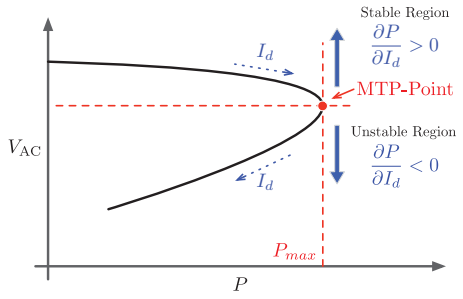

Fig. 5. PV-Curve and stability limit detection method

The uncontrolled AC voltage (V_{AC}) is at the receiving end of an AC transmission system. The voltage declines with increasing power up to the maximum transferable power (MTP) level, once the MTP-Point has been reached, it will decline with decreasing power. In general, this PV-curve holds also for an HVDC system being connected to an AC grid of moderate stiffness [8]. For the current control loop the upper branch is stable and the lower branch is unstable.

On the upper branch, DC current rises in proportion to the ordered DC power. If the MTP-Point is surpassed, the DC current continues to grow but the DC power declines. The conventional HVDC power controller is not able to detect this change, and the AC terminal voltage starts to collapse. The collapse can be halted through VDCOL. VDCOL does, however, not recognize if the system has already passed the stability border and that HVDC operates on the lower branch of the PV-curve. The Automatic Voltage Stabilizer (AVS) [7], [5], on the other hand, does not experience this problem. Essential for a statement on steady state stability is the sign of the quotient $\partial P/\partial Id$. AVS conceptualizes this derivative sign to distinguish between the upper and lower branch of the PV-curve and use it as a signal to trigger its operation. Since $\partial P/\partial Id$ cannot be measured directly, it is determined by measuring the derivatives $\partial P/\partial t$ and ∂I/∂t with respect to time, and forming the product of these derivatives resulting in: $\partial P/\partial t \times \partial I/\partial t$. If only one of the derivatives with respect to time becomes negative, which indeed occurs when moving along the lower branch of the PV-curve, the resulting derivative becomes negative. If both derivatives with respect to time are either positive or negative - which happens when the operating point moves along the upper branch - the product is positive, so we know that the operating point is on the upper branch. Therefore, we can use this signal to switch on AVS where the current level in the closed-loop current controller is adjustable so that the operating point is brought to the upper branch or revolve around the stability boundary which can be stopped by implementing the Automatic Power Order Reduction (APOR). This AVS and the APOR cover short-term as well as long term voltage instabilities whereby the first type of instability

occurs when the system's operating point moves suddenly to the lower branch of the PV-curve, e.g., through disconnecting lines or overexcitation limit (OEL) [9] and the second type of instability occurs, e.g., through slow changes of internal grid voltages. Figure 6 shows the PV-curve and voltage response at Bus 5 when one of the parallel line between Bus 1 and 3 is disconnected.

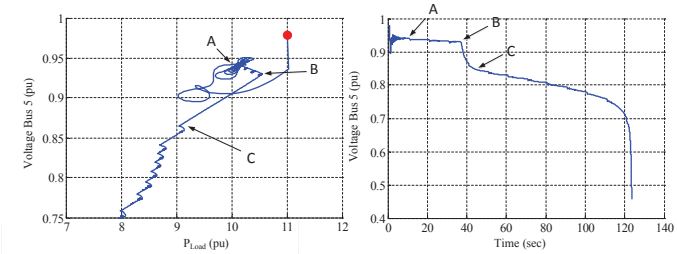

(a) PV-curve (b) Voltage at Bus 5

Fig. 6. PV-Curve and Voltage at Bus 5 - Line Trip Case

As seen from Fig 6 after one of the parallel lines is tripped, the system's equilibrium point moves from "red-dot" to point "A" to find a new equilibrium point. However, due to the operation of LTC that attempt to restore voltage at the lower voltage side of the transfer at the load bus, the voltage at higher side keeps decreasing. This triggers the OEL at the generator, thus generator voltage is no longer controlled. Consequently, this forces the system's operation point to jump from point "B" to point "C" which is the lower branch of the PV-curve. A similar process occurs with Classical HVDC working on a weak grid and transfer from DC voltage control to minimum extinction angle control [5].

IV. Case Studies

The AVS was implemented within the inverter control subsystem of the original CIGRÉ Benchmark model for (Classical) HVDC controls. The CIGRÉ Benchmark model was taken because it includes already all necessary inner and outer control loops of the converter and the converter pole and it provided the basis to implement a new stabilizing algorithm in an already verified environment. The algorithm was before tested in an own simpler setup and then transferred to the CIGRÉ Benchmark. The investigations were first done on the PSCAD/EMTDC digital simulator and then continued with the OPAL-RT simulator to include a more complex grid surrounding while avoiding excess computation time and to compare the performances of VDCOL with AVS and APOR. More details regarding the AVS and the APOR implementation can be found in [10]. Here additional case studies including a two-area system were conducted to elaborate further advantages of having AVS and APOR implemented within the HVDC.

A. Case I: Disconnection of AC line

If there is a radial system connecting the converter to the grid then a special signal is probably available to control the power order to stable values, provided proper design has taken place. In a meshed grid it might be difficult to provide this signal because of grid expansion or changes altering the conditions such that the original breaker trip detection system becomes invalid. Since the signal cannot be reliably provided other means are needed, the most important one the voltage dependent current order (VDCOL) limitation. The tuning of VDCOL is based on a SCR value = 3.3. However, there are incidents that the SCR becomes lower, e.g. AC line disconnection (the SCR value changes from 3.3 to 1.9, in this study) which results to an inappropriate VDCOL setting. In other words, the VDCOL function would not reliably prevent the operating point from jumping to the lower unstable PV-curve. However, if the VDCOL would be tuned for a SCR = 1.9 another problem would occur, namely: at normal operating conditions with only slightly decreased AC voltage the power would unnecessarily be curtailed. Moreover, it is not possible to discriminate between a normal voltage level and a voltage level indicating approaching instability.

Fig. 7 shows the oscillograms of the HVDC with the operation of the VDCOL and the AVS. It can be seen that an AC line is disconnected at time 8 sec resulting in a sudden voltage decline. Only the VDCOL is activated during t= 8-15 sec, which makes the voltage drop to 0.75 p.u.

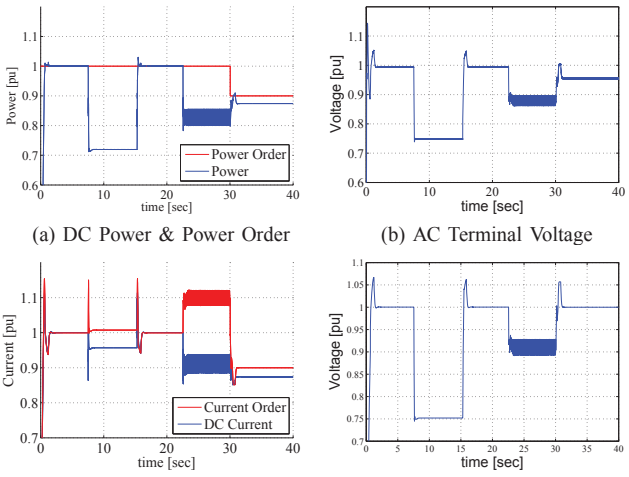

(a) DC Power & Power Order (b) AC Terminal Voltage

(c) DC Current & DC Current Order (d) DC Voltage

Fig. 7. Rectifier Oscillograms - HVDC with the AVS

Then the experiment is repeated by connecting and disconnecting an AC line at time 16 and 22 sec, respectively. However, in this case, the AVS is activated between t 22-30 sec, which retains the voltage level above 0.9 p.u. In order to increase the voltage level, the power reduction is activated at time 30 sec. Consequently, this brings the voltage back to 0.95 p.u. It is demonstrated that for the reduction of the SCR as given above the VDCOL cannot stop the shift over the nose of the PV-curve.

AVS operation makes the operating point revolve around the nose of the PV-curve. This nose determines the maximum transferable power. Of course, this kind of operation with periodically changing P- and Q-values is not desirable for a longer time. Therefore, the power can be reduced manually by the operator or automatically using APOR (it is done manually at 30 sec at this part of the article).

The next experiment is conducted to demonstrate the advantage of APOR over pure VDCOL. It can be seen in Fig. 8, as compared to the VDCOL function, APOR keeps the DC

voltage on a higher level and the DC current on a lower level while the power is actually higher. This is a clear indication that APOR keeps the operating point on the upper branch and VDCOL lets it slide to the lower branch meaning less efficiency and as we see later, also oscillations of power and transmission angle. This holds for slow changes of the power reference value exceeding the maximum transferable power level or when the internal grid voltage decreases gradually as well as for fast changes which occurs by disconnection of an AC line.

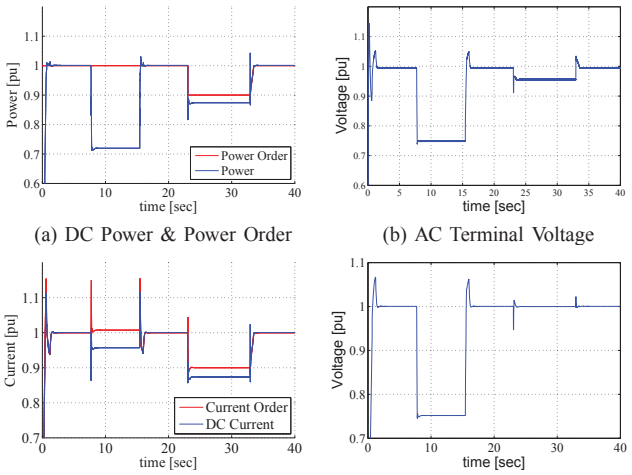

(a) DC Power & Power Order (b) AC Terminal Voltage

(c) DC Current & DC Current Order (d) DC Voltage

Fig. 8. Rectifier Oscillograms - HVDC with the APOR

B. Case II: Two-area AC system

In this case, we investigate the HVDC with the operation of the VDCOL and the APOR in a two-area AC transmission system. Fig. 9 shows the equivalent of two-area AC system which is connected at the rectifier side of the HVDC system. This two-area AC transmission system consists of a 500 MVA (local) generator and an 380 MVA induction machines in one area while another area is modeled as 1200 MVA (remote) generator. The local generator controls the AC terminal voltage of the rectifier as long as its excitation limit is not reached. The remote generator runs on proportional/integral speed control, the local generator on proportional speed control with an initial power ramp.

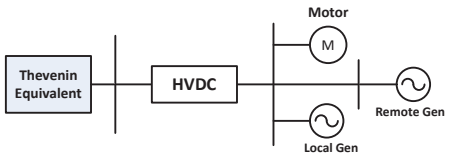

Fig. 9. Two-area AC system

The comparison study of HVDC with and without APOR is conducted by increasing the power consumption of the induction machine. As seen in Fig. 10, the active load of the induction machine is ramped up starting at time = 10 sec. In response to the AC terminal voltage decline the APOR mechanism is becoming active at t = 15 sec, which results in a small oscillation in the induction machine's electrical torque, afterwards this torque is held at constant until the active power of the induction machine is ramped down from t = 25 sec on. The same experiment is repeated at t = 40 sec, with only VDCOL being active. We recognize that VDCOL cannot prevent stalling of the induction machine.

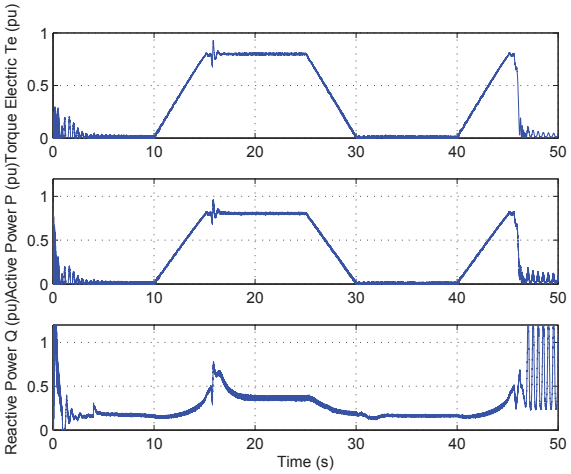

Fig. 10. Induction Machine Oscillograms

Fig 11 shows the oscillograms of the HVDC rectifier side. APOR, becoming active at time t = 15 sec, aids HVDC to hold a constant DC voltage by changing the power order which leads to a decrease of DC current. The reactive power consumption of the rectifier is decreased and also the reactive power demand of the AC line between the remote and local bus becomes smaller. This relieves the local generator somewhat from reactive power demand thus permitting the local generator to control again the AC terminal voltage.

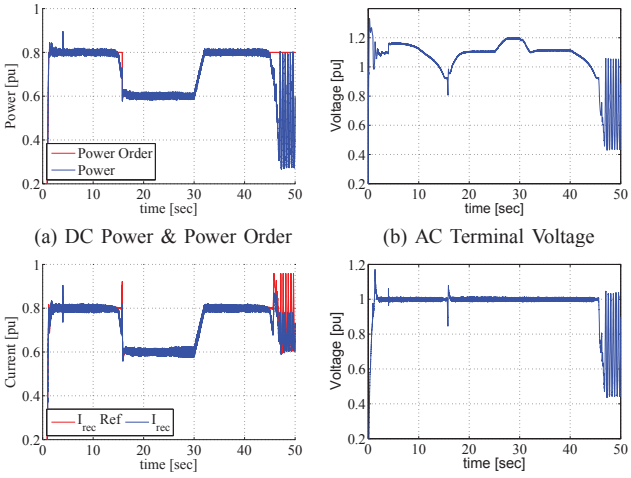

(a) DC Power & Power Order (b) AC Terminal Voltage

(c) DC Current & DC Current Order (d) DC Voltage

Fig. 11. Rectifier Oscillograms - HVDC with the APOR

Machine torque (Fig. 12) as well as transmission angle and power angle (Fig. 13) change in accordance with the power ramp of the induction machine and the speed control regime. There is no deviation from the expected results. Also a prediction made earlier [10] regarding power and angle swings when VDCOL cannot prevent that the nose of the PV-curve is surpassed can be confirmed (see Fig. 12 and 13 from

t = 45 sec on). However the oscillations are not normal two-area swings known from pure AC systems but result from DC power swings caused through unstable converter controls on the lower branch of the PV-curve. The reason for unstable controls is the transfer function's sign change of the plant to be controlled. As opposed to VDCOL the APOR function is able to prevent such swings by keeping the operating point on the upper branch of the PV-curve. Important to mention, although it is not part of this Section, that transmission systems with AC and DC in parallel can require an increase of DC power to stabilize a system. Also in this case the principle APOR function can be maintained by subtracting this time a negative value from the power order. The challenge is to determine whether an increase or a decrease of DC power is needed. A fundamental treatment of this problem can be found in [6].

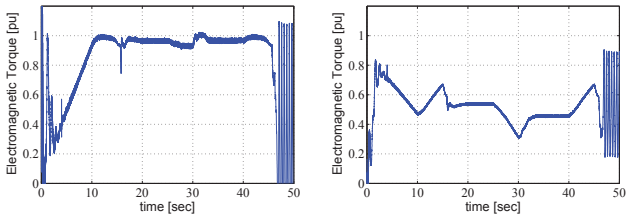

(a) Local Gen (b) Remote Gen

Fig. 12. Generators Torque

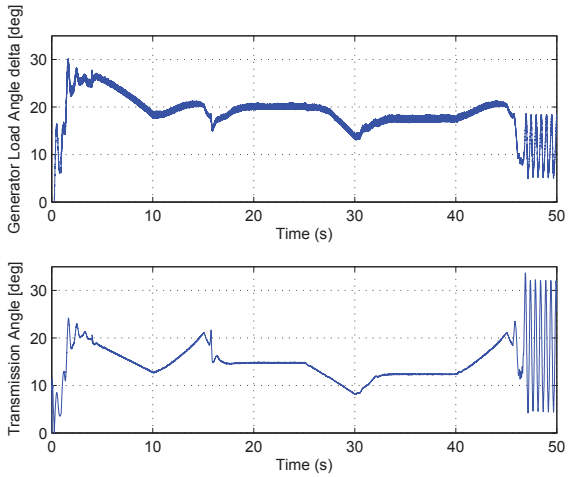

Fig. 13. Angles Remote Generator

V. Conclusion

This article purposes two approaches to prevent voltage instability. A system's impending voltage collapse can be detected by adopting the voltage sensitivities being determined from filtered synchrophasor data, in which errors and unnecessary features embedded in measurements are already corrected. Hence, the sensitivities are not only used for wide-area voltage monitoring but also for preventive action and cooperation with HVDCs.

There are however conditions and power flow situations where determination of sensitivities is not sufficient because their magnitudes do not permit a conclusive interpretation regarding the stability margin. This is, e.g. the case, if stiffness changes in a non-foreseeable manner (i.e. no study results on the necessary threshold values (in Section II) are available) or if at a given low stiffness HVDC controls cause discontinuities in sensitivity values. Then no safe indication of an impending voltage collapse via sensitivity calculation and their interpretation is possible. The latter being particularly the case when controllers hit suddenly unpredicted control limits, e.g. firing angle limits at rectifier operation or extinction angle at inverter operation. The present state of art to determine sensitivities on-line and to use them in real-time for grids including Classical HVDC is not yet advanced enough to ensure stability for obscured conditions. Further research is necessary combining sensitivity determination and HVDC system modeling to obtain continuously information on the distance to the stability boundary under inclusion of structural grid and load flow changes as well as grid internal and HVDC control limits.

Besides the voltage stability problem Classical HVDC systems are prone to electromechanical oscillations when embedded in AC systems with multiple-areas being primarily associated with a reversal of the sign of the transfer function of the "converter plant" when surpassing the nose of the PV-curve. Both voltage and electromechanical stability are presently not reliably ensured via the usually applied VDCOL function. Therefore, a real-time/on-line method was developed, implemented and tested in a CIGRÉ Benchmark model for HVDC controls. The obtained Automatic Voltage Stabilizer and the Automatic Power Order Reducer operate independently or in combination in stand-alone or to back-up non-reliably working stabilizing methods and implementations. The use of real-time simulators for this type of study has not only the benefit of allowing for faster computation times under inclusion of detailed controls, but also for the consideration of complex scenarios with multi-area AC grids and superimposed DC grids, distributed generation from renewable energy resources and bulk power transmission via AC and DC transmission systems.

References

[1] M. Glavic and T. Van Cutsem, "Investigating state reconstruction from scarce synchronized phasor measurements," in *2011 IEEE Trondheim PowerTech*, 2011.

[2] B. Milosevic and M. Begovic, "Voltage Stability Protection and Control using a Wide-Area Network of Phasor Measurements," *IEEE Transactions on Power Systems*, vol. 18, pp. 121–127, 2003.

[3] M. Glavic and T. Van Cutsem, "Wide-Area Detection of Voltage Instability From Synchronized Phasor Measurements. Part I: Principle," *IEEE Transactions on Power Systems*, vol. 24, pp. 1408–1416, 2009.

[4] O. I. Elgerd, *Electric Energy Systems Theory: An Introduction*, 2nd ed. McGraw-Hill Education - Europe, 1998.

[5] W. Kuehn, "Real-time method to prevent voltage collapse and power instability of HVDC systems," in *IEEE PES ISGT Europe*, 2010, pp. 1–8.

[6] A. E. Hammad, "Stability and Control of HVDC and AC Transmissions in Parallel," *IEEE Transactions on Power Delivery*, vol. 14, pp. 1545–1554, 1999.

[7] W. Kuehn, "Method and Apparatus for Automatic Network Stabilization in Electric Power Supply Systems using at least one converter," US Patent App. Pub. No.: US 2012/0112713 A1, Pub., May 2012.

[8] ——, "Control and Stability of Power Inverters Feeding Renewable Power to Weak AC Grids with No or Low Mechanical Inertia," in *IEEE PES PSCE09*, 2009, pp. 1–8.

[9] T. Van Custom and C. Vournas, *Voltage Stability of Electric Power Systems*. Kluwer Academic Publisher, 1998.

[10] K. Weyrich, "Integration of Renewable Energy Resources via Classic HVDC," B.Sc. Thesis, 2011.